

Oriented films of layered rare-earth hydroxide crystallites self-assembled at the hexane/water interface†

Linfeng Hu,^{ab} Renzhi Ma,^a Tadashi C. Ozawa,^a Fengxia Geng,^{ab} Nobuo Iyi^a and Takayoshi Sasaki^{*ab}

Received (in Cambridge, UK) 15th July 2008, Accepted 1st September 2008

First published as an Advance Article on the web 19th September 2008

DOI: 10.1039/b812111g

Layered rare-earth hydroxide crystallites self-assembled at the hexane/water interface were transferred to various substrates to form a monolayer film, which exhibited photoluminescence properties and ion-exchange ability.

Nanoparticle self-assembly into the form of oriented films on various substrates is an effective way to establish versatile functional entities, and has been a focus of interest during the past several decades.¹ Different approaches to nanoparticle assembly, such as solvent evaporation,² layer-by-layer assembly,³ the Langmuir–Blodgett method⁴ and spin-coating,⁵ have been developed. Recently, we synthesized a new layered rare-earth hydroxide with the composition $\text{Eu}(\text{OH})_{2.5}\text{Cl}_{0.5}\cdot 0.9\text{H}_2\text{O}$, which shows uniform rectangular platelet morphology with a size of several micrometres.⁶ This new layered compound displays anion-exchange behavior similar to that of a hydroxalcite-type layered double hydroxide (LDH),⁷ and also exhibits characteristic photoluminescence properties. The fabrication of film from these crystallites could hold great potential for various applications by combining the advantages of anion-exchange and the photoluminescence properties. However, traditional methods for film fabrication are not suitable for the $\text{Eu}(\text{OH})_{2.5}\text{Cl}_{0.5}\cdot 0.9\text{H}_2\text{O}$ crystallites, because they result in a poor quality film with low area coverage ratio and an abundant congeries of crystallites. Recently a monolayer film of Mg/Al-based LDH crystallites (size less than 500 nm) was fabricated by dipping the substrate into a suspension of LDH crystallites with ultrasonic treatment, and the LDH crystallites were immobilized by the bonding force between the positively-charged crystallites and the negatively-charged surface of the substrate.⁸ Nevertheless, this method cannot be applied to the $\text{Eu}(\text{OH})_{2.5}\text{Cl}_{0.5}\cdot 0.9\text{H}_2\text{O}$ crystallites, because the bonding force is not strong enough to immobilize the larger-sized crystallites on the substrate. Fabricating a high-quality film of micrometre-sized crystallites remains a challenge that requires a new approach.

Fluid/fluid interfaces are the ideal template for self-assembly of inorganic nanoparticles, and have received intensive

attention.⁹ Au, Ag, Pt, and SiO_2 nanoparticles and one-dimensional carbon nanotubes have been self-assembled at the toluene/water or hexane/water interfaces using ethanol as the inducer.¹⁰ The main driving force for this assembly is related to a decrease in interfacial energy of the nanoparticles caused by the addition of ethanol.¹¹ However, there are no reports on the assembly of micrometre-sized platelet crystallites by this simple approach. In this *communication*, we present a self-assembly procedure for preparing a monolayer film of layered rare-earth hydroxide crystallites at the hexane/water interface. After the film was transferred to a substrate, its photoluminescence and ion-exchange properties were studied.

In a typical experiment, 20 mg of $\text{Eu}(\text{OH})_{2.5}\text{Cl}_{0.5}\cdot 0.9\text{H}_2\text{O}$ crystallites were dispersed in 40 ml of Milli-Q water. Hexane (10 ml) was added to the vessel to produce a hexane/water interface. Next, ethanol (1.5 ml) was added to the interface at a low rate (0.6 ml min^{-1}), and the rare-earth hydroxide crystallites were immediately trapped at the interface. Then most of the hexane at the top of the vessel was carefully removed by syringe, and the densely packed film was transferred to a quartz or silicon substrate precoated with a polyanion (Fig. 1). After deposition, the film was immersed in ethanol with ultrasonic treatment for a few seconds, and then dried at room temperature to obtain a semitransparent monolayer film (Fig. S1, see ESI†). Multilayer films were fabricated by multiple repetition of the deposition process under the same conditions. Anion-exchange experiments were carried out by immersing a monolayer film into an aqueous solution of 1 M NaNO_3 and 0.5 M

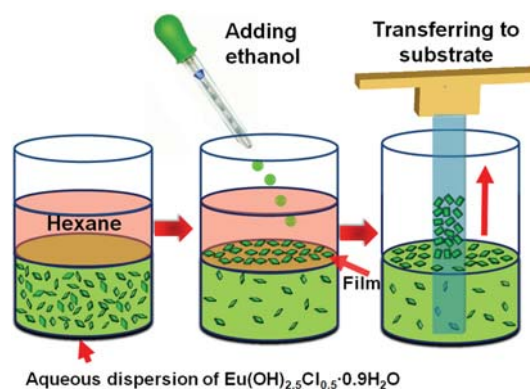


Fig. 1 Schematic representation of the monolayer formation for the $\text{Eu}(\text{OH})_{2.5}\text{Cl}_{0.5}\cdot 0.9\text{H}_2\text{O}$ crystallites at the hexane/water interface and the transfer procedure.

^a International Center for Materials Nanoarchitectonics and Nanoscale Materials Center, National Institute for Materials Science, 1-1 Namiki, Tsukuba, Ibaraki 305-0044, Japan.
E-mail: SASAKI.takayoshi@nims.go.jp; Fax: +81-29-854-9061;
Tel: +81-29-860-4313

^b Graduate School of Pure and Applied Sciences, University of Tsukuba, 1-1-1 Tennodai, Tsukuba, Ibaraki 305-8571, Japan

† Electronic supplementary information (ESI) available: Experimental details and SEM images of the films. See DOI: 10.1039/b812111g

sodium dodecylsulfate (SDS, $C_{12}H_{25}OSO_3Na$) for 72 h at room temperature.

Compared with the adhesion of crystallites on solid substrates by solvent evaporation, the present method produced a better-quality film with a higher area coverage ratio, which is shown in Fig. 2. It can be seen that the substrate is densely covered with the crystallites, although some small interspaces are inevitable, which may be attributed to the electrostatic repulsive force between the rare-earth hydroxide crystallites at the hexane/water interface.^{11a} Since the surface charge and interface energy of the crystallites at the interface are controlled by the amount of ethanol,^{9c} the addition of an appropriate quantity of ethanol is crucial for the formation of film with a desirable quality. Too little ethanol results in a low area coverage ratio, whereas too much ethanol leads to the obvious overlapping of crystallites as shown in Fig. S2.† Even with an optimal ethanol addition (*i.e.*, 1.5 ml in Fig. 2a and b), some aggregation of crystallites was still observed. A monolayer film without noticeable aggregation can be fabricated after suitable ultrasonic treatment (Fig. 2c and d), while mostly retaining the high area coverage ratio. The cavitation force generated by ultrasonic waves may remove the aggregation. For multilayer films, a high area coverage ratio and oriented arrangement of crystallites on the solid substrate are evident (Fig. S3†).

The highly preferred orientation of the crystallites immobilized on the substrate can be confirmed by the X-ray diffraction (XRD) pattern, as shown in Fig. 3b. Compared with the XRD pattern for the powder sample in Fig. 3a, only 00/ diffraction peaks can be detected for the monolayer film. Moreover, the diffraction peaks in Fig. 3b are much higher in intensity than those of the powder sample. These results demonstrate that all the crystallites in the film are aligned on the substrate with their *c*-axis perpendicular to the substrate surface.

Excitation and emission spectra of the multilayer films at room temperature are shown in Fig. 4a and b, respectively, which exhibit no apparent differences compared with those of the powder sample. The excitation spectra consist of a series of

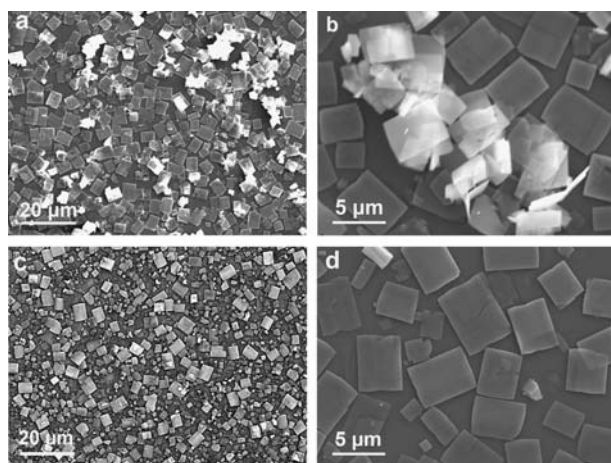


Fig. 2 Typical SEM images of the film of $Eu(OH)_{2.5}Cl_{0.5} \cdot 0.9H_2O$ platelet crystallites on a Si substrate (a, b) before and (c, d) after ultrasonic treatment. Bright portions correspond to aggregation of crystallites.

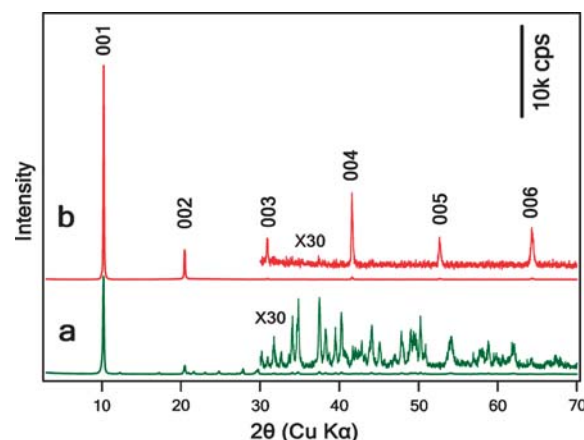


Fig. 3 XRD patterns for (a) powder sample of $Eu(OH)_{2.5}Cl_{0.5} \cdot 0.9H_2O$; (b) monolayer film of $Eu(OH)_{2.5}Cl_{0.5} \cdot 0.9H_2O$ crystallites. (Inset) Enlarged view of the patterns from a high angle.

sharp lines ascribed to the intra- $4f^6$ transitions within the electronic configuration of $Eu^{3+} 4f^6$. The emission spectra display typical ${}^5D_0-{}^7F_J$ ($J = 0-4$) transitions at 579.8, 595.2, 615.4, 651.2, and 701.1 nm, respectively.⁶ The intensity of the emission peak at 701 nm increases roughly in proportion to the number of layers. The photoluminescence properties of the multilayer films can also be confirmed by the red-emission

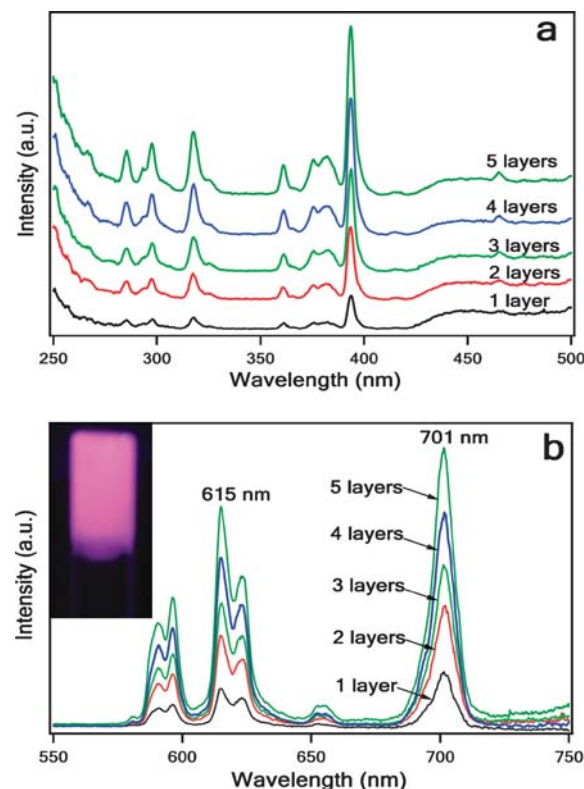


Fig. 4 Photoluminescence (a) excitation spectra monitored at 615 nm and (b) emission spectra excited at 393 nm of the $Eu(OH)_{2.5}Cl_{0.5} \cdot 0.9H_2O$ multilayer films. The inset in (b) shows the red-light emission of the tri-deposited multilayer film under UV irradiation (the weak violet color at the edge of the film is caused by the violet components of the incident light of the UV lamp).

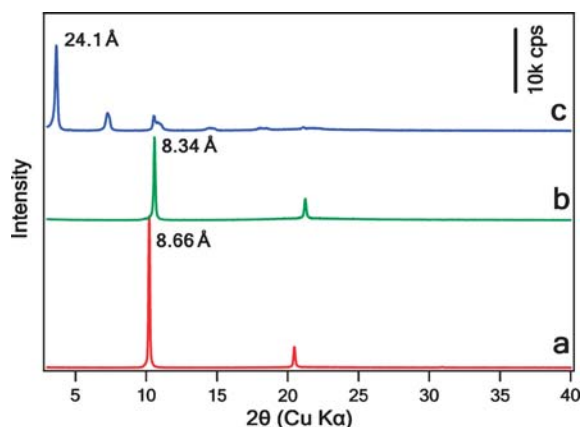


Fig. 5 XRD patterns of the monolayer film: (a) Cl^- form before ion-exchange; (b) NO_3^- form after ion-exchange; (c) $\text{C}_{12}\text{H}_{25}\text{OSO}_3^-$ form after ion-exchange.

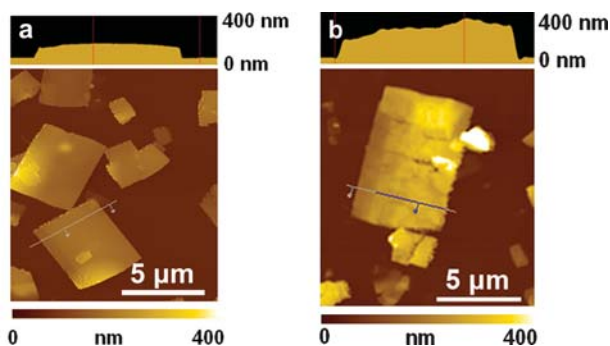


Fig. 6 Typical AFM images of (a) pristine Cl^- form crystallites and (b) the crystallites after ion-exchange with $\text{C}_{12}\text{H}_{25}\text{OSO}_3^-$ ions.

photograph under UV irradiation of the three-layer film, as shown in the inset in Fig. 4b.

Fig. 5 shows the XRD patterns of the monolayer film before and after anion-exchange reactions. The basal spacing, 8.66 Å for the pristine Cl^- form, shifts to 8.34 Å for the NO_3^- form and 24.1 Å for the $\text{C}_{12}\text{H}_{25}\text{OSO}_3^-$ form. The sharp diffraction peaks demonstrate that the high crystallinity and oriented arrangement of the rare-earth hydroxide crystallites can be maintained during the ion-exchange process. The monolayer film of Mg/Al-based LDH nanocrystals reported by Lee *et al.* shows anion-exchange capacity under solvothermal treatment.⁸ In contrast, the current monolayer of $\text{Eu}(\text{OH})_{2.5}\text{Cl}_{0.5}\cdot 0.9\text{H}_2\text{O}$ is readily anion-exchangeable at room temperature, which is simpler and more desirable.

Fig. 6 displays the atomic force microscopy (AFM) images of the rare-earth hydroxide crystallites before and after ion-exchange with $\text{C}_{12}\text{H}_{25}\text{OSO}_3^-$ ions. It is apparent that the rectangular platelet morphology of the crystallites is well retained during the reaction. The crystallites show a smooth surface for the pristine Cl^- form, but the surface becomes rather rough after ion-exchange with $\text{C}_{12}\text{H}_{25}\text{OSO}_3^-$ ions. The

average height of the crystallites was obtained based on statistical examination of more than 30 crystallites (Fig. S4†). The average height of Cl^- and $\text{C}_{12}\text{H}_{25}\text{OSO}_3^-$ crystallites measured 101 ± 33 and 267 ± 62 nm, respectively, indicating expansion by 2.7 times, which is consistent with the change in basal spacing in the XRD data.

In summary, a simple method for organizing densely packed monolayer and multilayer films of new layered rare-earth hydroxide crystallites has been developed. The film of $\text{Eu}(\text{OH})_{2.5}\text{Cl}_{0.5}\cdot 0.9\text{H}_2\text{O}$ platelet crystallites exhibits typical photoluminescence properties and excellent anion-exchange behavior, and may have potential applications in optical devices *etc.*

This work has been supported by CREST of the Japan Science and Technology Agency (JST) and World Premier International Center Initiative (WPI Initiative) on Materials Nanoarchitectonics, MEXT, Japan.

Notes and references

- (a) M. Li, H. Schnablegger and S. Mann, *Nature*, 1999, **402**, 393; (b) J. H. Lee, S. W. Rhee and D. Y. Jung, *J. Am. Chem. Soc.*, 2007, **129**, 3522.
- K. Okamoto, T. Sasaki, T. Fujita and N. Iyi, *J. Mater. Chem.*, 2006, **16**, 1608.
- (a) R. Ma, T. Sasaki and Y. Bando, *J. Am. Chem. Soc.*, 2004, **126**, 10382; (b) A. Javey, S. W. Nam, R. S. Friedman, H. Yan and C. M. Lieber, *Nano Lett.*, 2007, **7**, 773.
- (a) X. L. Li, L. Zhang, X. R. Wang, I. Shimoyama, X. M. Sun, W. S. Seo and H. J. Dai, *J. Am. Chem. Soc.*, 2007, **129**, 4890; (b) A. Tao, P. Sinsersuksakul and P. D. Yang, *Nat. Nanotech.*, 2007, **2**, 435.
- (a) A. Mihi, M. Ocaña and H. Míguez, *Adv. Mater.*, 2006, **18**, 2244; (b) T. Shibata, K. Fukuda, Y. Ebina, T. Kogure and T. Sasaki, *Adv. Mater.*, 2008, **20**, 231.
- F. X. Geng, H. Xin, Y. Matsushita, R. Ma, M. Tanaka, F. Izumi, N. Iyi and T. Sasaki, *Chem.–Eur. J.*, 2008, DOI: 10.1002/chem.200800127.
- (a) Z. P. Liu, R. Ma, M. Osada, N. Iyi, Y. Ebina, K. Takada and T. Sasaki, *J. Am. Chem. Soc.*, 2006, **128**, 4872; (b) R. Ma, K. Takada, K. Fukuda, N. Iyi, Y. Bando and T. Sasaki, *Angew. Chem., Int. Ed.*, 2008, **47**, 86; (c) L. Li, R. Ma, Y. Ebina, N. Iyi and T. Sasaki, *Chem. Mater.*, 2005, **17**, 4386.
- (a) J. H. Lee, S. W. Rhee and D. Y. Jung, *Chem. Commun.*, 2003, 2740; (b) J. H. Lee, S. W. Rhee and D. Y. Jung, *Chem. Mater.*, 2004, **16**, 3774; (c) J. H. Lee, S. W. Rhee and D. Y. Jung, *Chem. Mater.*, 2006, **18**, 4740.
- (a) Y. Lin, H. Skaff, T. Emrick, A. D. Dinsmore and T. P. Russell, *Science*, 2003, **299**, 226; (b) H. W. Duan, D. Y. Wang, D. G. Kurth and H. Möhwald, *Angew. Chem., Int. Ed.*, 2004, **43**, 5639; (c) F. Reincke, S. G. Hickey, W. K. Kegel and D. Vanmaekelbergh, *Angew. Chem., Int. Ed.*, 2004, **43**, 458.
- (a) Y. J. Li, W. J. Huang and S. G. Sun, *Angew. Chem., Int. Ed.*, 2006, **45**, 2537; (b) S. Yun, Y. K. Park, S. K. Kim and S. Park, *Anal. Chem.*, 2007, **79**, 8584; (c) J. Wang, D. Y. Wang, N. S. Sobal, M. Giersig, M. Jiang and H. Möhwald, *Angew. Chem., Int. Ed.*, 2006, **45**, 7963; (d) Y. K. Park, S. H. Yoo and S. Park, *Langmuir*, 2007, **23**, 10505; (e) J. Matsui, K. Yamamoto, N. Inokuma, H. Orikasa, T. Kyotani and T. Miyashita, *J. Mater. Chem.*, 2007, **17**, 3806.
- (a) F. Reincke, W. K. Kegel, H. Zhang, M. Nolte, D. Y. Wang, D. Vanmaekelbergh and H. Möhwald, *Phys. Chem. Chem. Phys.*, 2006, **8**, 3828; (b) S. Kutuzov, J. He, R. Tangirala, T. Emrick, T. P. Russell and A. Böker, *Phys. Chem. Chem. Phys.*, 2007, **9**, 6351.